GRB Fireball Physics: Prompt and Early Emission

D. B. Fox & P. Mészáros

Dept. of Astronomy & Astrophysics and Dept. of Physics, Pennsylvania State University, University Park, PA 16802, USA

Abstract. We review the fireball shock model of gamma-ray burst prompt and early afterglow emission in the light of rapid follow-up measurements made and enabled by the multi-wavelength *Swift* satellite. These observations are leading to a reappraisal and expansion of the previous standard view of the GRB and its fireball. New information on the behavior of the burst and afterglow on minutes to hour timescales has led, among other results, to the discovery and follow-up of short GRB afterglows, the opening up of the $z \gtrsim 6$ redshift range, and the first prompt multi-wavelength observations of a long GRB-supernova. We discuss the salient observational results and some associated theoretical issues.

1. Observational Advances in the Swift Era

NASA's *Swift* mission [1] has enabled fundamental insights into the physics of gamma-ray bursts thanks to two new capabilities: First, the greater sensitivity of its Burst Alert Detector [2] (BAT; energy range 20–150 keV) in comparison to the preceding *Beppo-SAX* and *HETE-2* missions [3]; and second, its ability to slew in less than 100 seconds to the burst direction determined by the BAT, which allows it to position its much higher-angular resolution X-ray (XRT, few-arcsec) and UV-Optical (UVOT, sub-arcsec) detectors [4, 5] for observations of the prompt and early afterglow emission.

As of July 2006, over 150 bursts had been detected by BAT, at an average rate of 2 bursts detected per week. Of these, roughly 90% were followed promptly with the XRT within 350 s from the trigger, and about half within 100 s [6], while $\sim 30\%$ were detected with the UVOT [7]. This resulted in over 30 new redshift determinations. Eleven definitive short GRBs were detected, of which seven had detected X-ray afterglows (including three with optical afterglows, and two with radio), and five had proposed redshifts.

These *Swift* observations, complemented by the continuing operations of the *HETE-2* and *INTEGRAL* missions, have brought the total number of redshift determinations to over 60 since *Beppo-SAX* enabled the first one in 1997. The redshifts based on *Swift* have a median $z \sim 2.8$ [8, 9], which is a factor $\gtrsim 2$ higher than the median of those previously culled via *Beppo-SAX* and *HETE-2* [10]. This can be credited largely to the prompt ∼arcsec positions from XRT and UVOT, which make rapid ground-based observations possible at a stage when the afterglow is still bright. The highest *Swift*-enabled redshift so far was that of GRB 050904, from 8-meter class Subaru spectroscopy, $z = 6.29$ [11] (the pre-*Swift* record was $z = 4.5$ for the IPN-localized GRB 000131 [12]). The relative paucity of UVOT detections versus XRT detections may be ascribed in part to this higher median redshift (and correspondingly reduced median flux), and in part to the (expected) increased dust extinction at the shorter rest-frame wavelengths implied for any given observing band [7], although the issue is still the subject of debate.

BAT light curves: The BAT is provided with an array of triggering algorithms which provide greater sensitivity than those of previous spacecraft, including "imaging" triggers which, through analysis of the counts integrated over 128-s to 512-s timescales, enable the detection of faint, slow-rising events. In a peculiar irony of GRB studies, these image triggers have made possible the discovery of both the farthest, highly time-dilated burst GRB 050904, and the nearest, faint and slow-rising burst GRB 060218 (see below for further discussion). For some of the bursts which fall in the "long" category (γ-ray duration $t_\gamma \gtrsim 2$ s), the BAT has detected faint soft gamma-ray tails which extend the duration by a factor up to two beyond what the previous Burst and Transient Source Experiment (BATSE) could have detected [13]. Such extended soft tails have been found also in some "short" bursts, normally defined as having a hard spectrum and duration $t_\gamma \lesssim 2$ s (see below).

XRT light curves: Striking new insights into burst and afterglow physics have come

from the detailed X-ray light curves, starting on average 100 seconds after the γ-ray trigger, that result from the prompt XRT observations of BAT-detected bursts. These observations suggest a canonical X-ray afterglow (Fig. 1; [14, 15]) with one or more of the following stages (note that the numerical subscript enumerates each stage): (1) An initial steep decay $F_X \propto t^{-\alpha_1}$ with temporal index $3 \lesssim \alpha_1 \lesssim 5$, and an energy spectrum $F_\nu \propto \nu^{-\beta_1}$ with energy spectral index $1 \lesssim \beta_1 \lesssim 2$ (photon index $0 \lesssim \Gamma \lesssim 1$), extending up to a time $300\,\mathrm{s} \lesssim t_1 \lesssim 500\,\mathrm{s}$; (2) A subsequent flatter decay $F_X \propto t^{-\alpha_2}$ with $0.2 \lesssim \alpha_2 \lesssim 0.8$ and energy index $0.7 \lesssim \beta_2 \lesssim 1.2$, at times $10^3\,\mathrm{s} \lesssim t_2 \lesssim 10^4\,\mathrm{s}$ (in some cases interspersed with flares, see [15]; (3) A "normal" decay $F_X \propto t^{-\alpha_3}$ with $1.1 \lesssim \alpha_3 \lesssim 1.7$ and $0.7 \lesssim \beta_3 \lesssim 1.2$ (generally unchanged from the previous stage, i.e. $\beta_3 \approx \beta_2$), up to a time $t_3 \sim 10^5\,\mathrm{s}$, or in some cases longer; (4) In some cases, a steeper X-ray decay at the end, $F_X \propto t^{-\alpha_4}$, with $2 \lesssim \alpha_4 \lesssim 3$, after $t_4 \sim 10^5\,\mathrm{s}$, resembling what is expected from jet breaks; (5) In about half the afterglows, one or more X-ray flares or bumps are observed in the light curve, sometimes starting as early as 100 s after trigger, and sometimes as late as $10^5\,\mathrm{s}$. The energy in these flares ranges from a percent up to a value comparable to the prompt emission (in GRB 050502b). The rise and decay times of these flares is unusually steep, depending on the reference time t_0, behaving as $(t - t_0)^{\pm\alpha_{\rm fl}}$ with $3 \lesssim \alpha_{\rm fl} \lesssim 6$, and energy indices which can be also steeper than during the smooth decay portions. The flux level after the flare usually decays to the value extrapolated from the value before the flare rise.

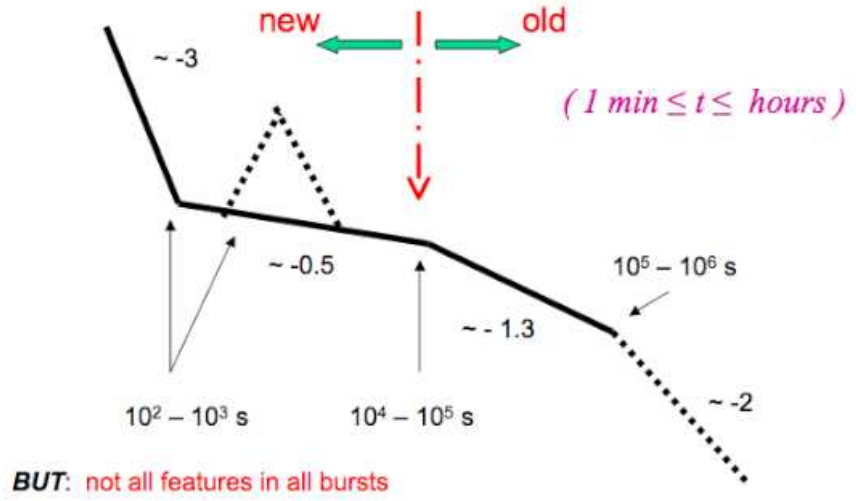

Figure 1. Schematic features seen in early X-ray afterglows detected with the *Swift* XRT instrument (e.g. [15, 14]); see text.

Very high-redshift bursts: Another major advance achieved by *Swift* was the detection of the long burst GRB 050904, which broke the $z > 6$ redshift barrier. This burst was very bright, both in its prompt γ-ray emission ($E_{\gamma,\rm iso} \sim 10^{54}$ erg) and in its X-ray afterglow. Prompt ground-based optical/IR upper limits and a J-band detection suggested a photometric redshift $z > 6$ [16]. Spectroscopic confirmation with the 8.2 m Subaru telescope gave $z = 6.29$ [11]. There are several striking features to this burst.

One is its enormous X-ray brightness, exceeding for a full day the X-ray brightness of the most distant quasar known to-date, SDSS J0130+0524 – and exceeding it by a factor of 10^5 in the first minutes [17]. The implications for the use of GRBs as a tool for probing the IGM are thought-provoking. Another notable feature was its extremely variable X-ray light curve, showing many large amplitude flares throughout the first day (Fig. 2). A third exciting feature is its brief, very bright IR flash [18], comparable in brightness to the famous $m_V \sim 9$ optical flash in GRB 990123.

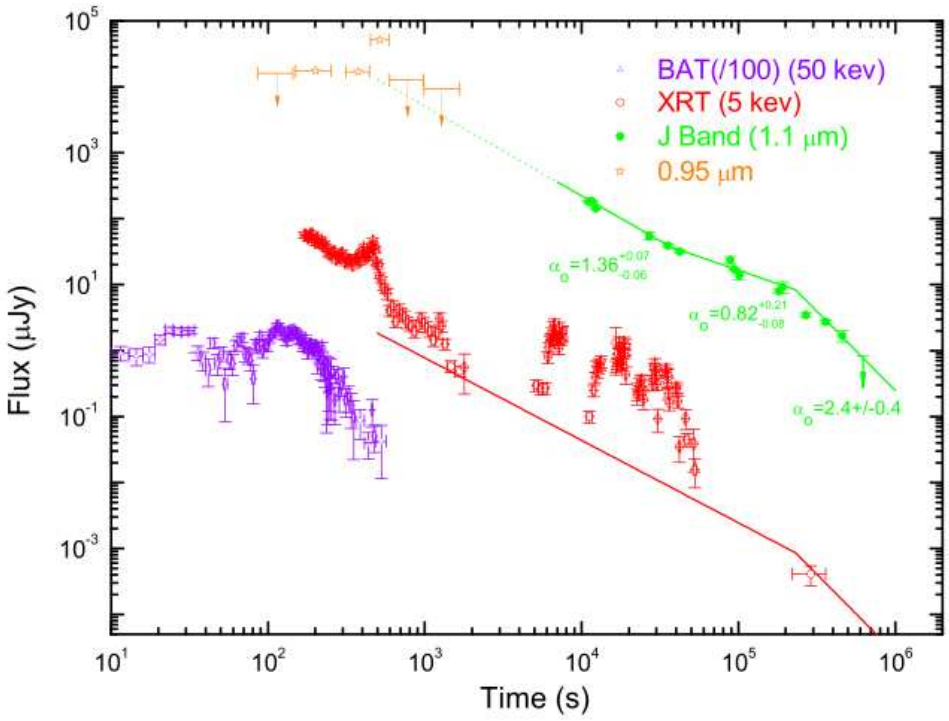

Figure 2. Prompt and afterglow lightcurves for the redshift $z = 6.29$ GRB 050904 at hard X-ray (BAT, 50 keV), X-ray (XRT, 5 keV), and near-infrared (J-band, 1.1 μm; and I-band, 9500 Å) frequencies. A bright early flare is seen in the IR and X-ray; in the X-ray this is followed by extensive flaring activity for more than a day after the burst. Power-law decay indices measured in the IR (α_o) are indicated, where available; a likely jet break is seen at $t \approx 2.3$ days [20]. Data from [16, 18, 19, 20].

Short bursts: The third major advance from *Swift* was the discovery and localization of short GRB afterglows. As of July 2006, eleven definitive short bursts have been localized by *Swift*, and *HETE-2* has discovered two short bursts with subsequent afterglow emission; in addition, the short burst GRB 051103 was localized by the IPN to a region intersecting the nearby galaxies M81 and M82. In seven of the *Swift* short bursts and two *HETE-2* bursts an X-ray afterglow was detected and observed, with GRBs 050709, 050724, 051221A, 060313, and 060121 (as well as the candidate short burst GRB 051227) also showing optical afterglows, and GRBs 050724 and 051221A being detected in the radio [21]. These are the first afterglows detected for short bursts, and yielded the first host galaxy identifications. The hosts are of early type (ellipticals) in roughly half the cases, and otherwise appear to be dwarf irregular galaxies – albeit

with evidence for old as well as young stellar populations [22]. The redshifts of five of them are in the range 0.15 to 0.5, while GRB 050813 was initially thought to have $z = 0.7$ [23] but may be associated with a galaxy cluster at $z \approx 1.8$ [21], and the redshift of the *HETE-2* GRB 060121 is estimated to be $z \approx 4.6$ [24]. The median z (as yet unaffected by these two relatively high redshifts) is $z_{\rm med} = 0.26$, which gives a $(1 + z)$ that is 1/3 that of the long bursts. While there is evidence for star formation in roughly half the host galaxies, overall the host properties correspond to expectations for a progenitor population of neutron star or neutron star-black hole binary systems, the most often-discussed progenitor candidates. Such hosts would also be compatible with other progenitors involving old compact stars.

The first short burst afterglow seen by *Swift* was that of GRB 050509B, a low luminosity ($E_{\gamma,\rm iso} \sim 2 \times 10^{48}$ erg) burst with a simple power-law X-ray afterglow which could only be followed for $\sim 10^4$ s [25]. The subsequent afterglows of GRB 050724 ($E_{\gamma,\rm iso} \sim 3 \times 10^{50}$ erg; [26]) and GRB 051221A ($E_{\gamma,\rm iso} \sim 1.5 \times 10^{51}$ erg; [22]) were brighter, and could be followed in X-rays for at least 10^5 s [27, 28]. In particular, the X-ray afterglow of GRB 050724 is remarkable in that it exhibits a typical X-ray light curve as observed from long GRBs by *Swift* (apart from the absence of a slow-decay phase). It shows a fast early decay, with significant X-ray flares, one at 100 s and another at 3×10^4 s. The first flare has the same fluence as the prompt emission, while the late flare has roughly 10% of that. The interpretation of this activity poses interesting challenges, as discussed below.

The GRB-SN connection: The fourth major advance from *Swift* was its observation, with BAT, XRT and UVOT, of an unusually long (~ 2000 s), soft burst, GRB 060218 [29], soon found to be associated with SN2006aj, a nearby ($z = 0.033$) type Ic supernova [30, 31, 32, 33]. The optical light curve of this supernova peaked earlier than for most other known supernovae, and the time of core collapse is constrained to within a day of the GRB trigger. This was the first time that a connected GRB and supernova event was observed starting in the first ∼100 s in X-ray and UV/optical light, and the results are of great interest. The early X-ray light curve shows a slow rise and plateau followed by a drop after $\sim 10^3$ s; the spectrum is initially dominated by a power-law component, with an increasing thermal component that dominates after ≈3000 s. Perhaps the most interesting interpretation involves shock break-out of a semi-relativistic component in a WR progenitor wind [29], although see also [34]. After this a more conventional X-ray power-law decay follows, and a UV component peaking at a later time can be interpreted as due to the slower supernova envelope shock. Finally, a radio-bright component is seen that presents an interesting comparison to other local and GRB-related type Ic supernovae [33]. A distinct GRB/SN detection based on *Swift* afterglow observations is that associated with GRB 050525A [35].

Prompt optical observations: A final major advance enabled by *Swift* has been a wealth of information about the prompt and early-time optical emission of GRBs. Thanks to *Swift* alerts and an array of ground-based robotic telescopes (as well as the UVOT), the detection of optical counterparts during and shortly after (<100 s)

the gamma-ray trigger is becoming almost routine. The *Swift* era began with the detection in optical [36] and near-infrared [37] wavelengths of a bright flash associated with GRB 041219A (localized in real time by *INTEGRAL*). Apart from exhibiting the first optical flash with brightness (after correcting for Galactic extinction) similar to GRB 990123, this burst showed the first evidence for correlated low- and high-energy emission, intepreted as optical emission from the same internal shocks that produced the GRB [36, 37]. A similar level of correlated optical emission was later observed from GRB 050820A [38]; however in this case it was accompanied by an uncorrelated component that connected smoothly to the later afterglow. Prompt optical emission that extrapolates smoothly to the later afterglow seems to be the more usual case; however, bright flares consistent with a reverse-shock interpretation are seen on occasion [39, 40]. The most exciting single observation is probably the $I = 14.1$ mag optical flash from GRB 050904 at $z = 6.3$ observed with TAROT [18], which rises to its peak after the end of gamma-ray emission and is brighter, and decays more quickly than, the later afterglow – all properties consistent with an origin in this burst's reverse shock.

2. Prompt Emission Models

The prompt gamma-ray emission of a classical GRB has most of its energy in the energy range 0.1 to 2.0 MeV. The generic photon spectrum is a broken power law [41] with a break energy in the above range, and, typically, power law extensions down into the X-ray, and up into the 100 MeV to GeV ranges (although a number of bursts show a thermal-like spectrum, which sometimes can be fitted with a blackbody [42]).

2.1. Gamma-Ray Emission

The simplest model for the gamma-ray emission assumes that a proton crossing a strong shock front with a relative bulk Lorentz factor Γ_{21} acquires (in the comoving frame) an internal energy characterized by a random (comoving) Lorentz factor $\gamma_{p,m} \sim \Gamma$ [43]. The comoving magnetic field behind the shock can build up due to turbulent dynamo effects behind the shocks [43, 44] (as also inferred in supernova remnant shocks). More recently, the Weibel instability has been studied in this context [45, 46, 47]. The efficiency of this process remains under debate, but one can parametrize the magnetic field as having a post-shock energy density which is a fraction ϵ_B of the equipartition value relative to the proton random energy, $B' \sim [32\pi\epsilon_B n_{ex}(\gamma'_p - 1)m_p c^2]^{1/2}\Gamma$, where the post-shock proton comoving internal energy is $(\gamma'_p - 1)m_p c^2 \sim 1$ (or $\sim \Gamma$) for internal (external) shocks [43, 48]. Scattering of electrons (and protons) by magnetic irregularities upstream and downstream can lead to a Fermi acceleration process resulting in a relativistic power law distribution of energies $N(\gamma) \propto \gamma^{-p}$ with $p \geq 2$. The starting minimum (comoving) Lorentz factor of the thermal electrons injected into the acceleration process, $\gamma_{e,m}$ would in principle be the same as for the protons, Γ (they experience the same velocity difference), hence both before and after acceleration they would have $\sim (m_e/m_p)$

less energy than the protons. However, the shocks are collisionless, i.e. mediated by chaotic electric and magnetic fields, and can redistribute the proton energy between the electrons and protons, up to some fraction ϵ_e of the thermal energy equipartition value with the protons, so $\gamma_{e,m} \sim \epsilon_e(m_p/m_e)\Gamma$ [44, 49]. The synchrotron spectrum, in its simplest form, peaks at $\nu_m \sim \Gamma(3/8\pi)(eB'/m_e c)\gamma_m^2 \sim 2\times 10^6 B'\gamma_m^2\Gamma$ Hz, and has a shape $F_\nu \propto [\nu^{1/3};\ \nu^{-(p-1)/2}]$ for $[\nu < \nu_m;\ \nu > \nu_m]$, in the adiabatic limit where the cooling time is longer than the dynamic time. In the opposite (radiative) limit, the spectrum peaks at the cooling frequency ν_c (at which cooling time for electrons emitting at ν_c equals dynamic time, and the spectrum above is $F_\nu \propto \nu^{-p/2}$. Depending on the parameters, more complicated spectra are possible, discussed e.g. in [50]. The synchrotron spectrum is modified at low energies by self-absorption [44, 51], making the spectrum steeper; and it is also modified at high energies, due to inverse Compton effects [44, 49, 52], extending into the GeV range.

However, a number of effects can modify the simple synchrotron spectrum. For instance, the distribution of observed low energy spectral indices β_1 (where $F_\nu \propto \nu^{\beta_1}$ below the spectral peak) has a mean value $\beta_1 \sim 0$, but for a fraction of bursts this slope reaches positive values $\beta_1 > 1/3$ which are incompatible with a simple synchrotron interpretation [53]. Possible explanations include synchrotron self-absorption in the X-ray [54] or in the optical range up-scattered to X-rays [55], low-pitch angle scattering or jitter radiation [56, 57], observational selection biases [58] and/or time-dependent acceleration and radiation [59], where low-pitch angle diffusion can also explain high energy indices steeper than predicted by isotropic scattering. Other models invoke a photospheric component and pair formation [60]. Pair formation can become important in internal shocks or dissipation regions occurring at small radii, since a high comoving luminosity implies a large comoving compactness parameter. A moderate to high scattering depth can lead to a Compton equilibrium which gives spectral peaks in the right energy range [61, 62]. An important aspect is that Compton equilibrium of internal shock electrons or pairs with photospheric photons leads to a high radiative efficiency, as well as to spectra with a break at the right preferred energy and steep low energy slopes [63, 64, 65]. It also leads to possible physical explanations for the Amati [66] or Ghirlanda [67] relations between spectral peak energy and burst fluence [63, 68].

2.2. Optical Emission

Prompt optical flashes, defined as optical emission detected while gamma-ray emission is still in progress and exemplified by the original detection from GRB 990123 [69], have been generally interpreted [70, 71, 72] as radiation from the reverse component of the external shock. However, a prompt optical flash can be produced from either an internal shock or the reverse external shock, or both [73, 71]. The decay rate of the optical flux from reverse shocks is very fast (and that of internal shocks, faster yet) compared to the decay of forward shock emission, so that the forward shock component typically dominates within minutes to tens of minutes.

Observations prior to the *Swift* era demonstrated already that bright flashes such as that seen from GRB 990123 were relatively rare. At the same time, the slow-fading ($\alpha \sim 0.4$) optical emission from GRB 021004 and the relatively faint optical flash from GRB 021211 were both argued to have properties consistent with a reverse shock origin [74, 75, 76, 77, 78, 79].

Optical/UV afterglows are now detected at early times, <100 s, in prompt observations with the *Swift* UVOT telescope in roughly half the bursts for which an X-ray afterglow was seen; for a detailed discussion see [7]. Of particular interest is the ongoing discussion of whether the "dark GRBs" which remain undetected by the UVOT are really optically deficient, or remain unobserved due to observational biases (e.g., the relatively blue bandpass of UVOT and the high redshifts of the *Swift* sample; [10]).

The fastest routine responses to *Swift* alerts are being realized by robotic ground-based telescopes, a large number of which have been brought on-line in recent years. The first substantial discovery yielded by these observatories has been of the gamma-ray correlated component of the prompt optical emission [36, 37, 38]. This component is not observed in every burst, but the mere fact of this correlation is sufficient to establish its likely origin in the burst's internal shocks [73, 71]. When observed, the ratio of the correlated gamma-ray to optical flux densities has been found to be roughly 10^5 to one.

In contrast to bursts with reverse-shock flare or gamma-ray correlated emission, the typical burst is now revealed to either exhibit a single power-law decay from early times [80, 81, 82], or to exhibit a flat or rising light curve [83, 84] before it enters the standard power-law afterglow decay. The initial brightness of the typical counterpart is $V \sim 14$ to 17 mag, which has made observations challenging for the usual <1 m telescopes employed.

There are a number of possible reasons for the observed faintness of early optical emission from typical GRBs. Suppression of internal shock emission can be provided by self-absorption in the optical, coupled to the lower flux implied by the $\nu^{1/3}$ low-energy asymptote of the synchrotron spectrum peaking at $\sim$ MeV [73]. Suppression of reverse shock emission, on the other hand, may indicate the absence or weakness of the reverse shock, e.g. if the ejecta are highly magnetized [73]. Alternatively, the deceleration might occur in the thick-shell regime ($T \gg t_{dec}$), resulting in the reverse shock being relativistic and boosting the optical spectrum into the UV [85] (but a detection by UVOT might then be expected, unless the decay is faster than the typical 100 to 200 s UVOT response time). Another possibility, for a high comoving luminosity, is copious pair formation in the ejecta, causing the reverse shock spectrum to peak in the IR [86]. Both GRBs 990123 and 050904 (see below) have a relatively large $E_{\gamma,\rm iso} \sim 10^{54}$ erg, so the latter seems a promising option. Even without pairs, more accurate calculations of the reverse shock [87, 88] find the emission to be significantly weaker than what was estimated earlier. Yet another possibility is that the cooling frequency in reverse shock is not much larger than the optical band frequency. In this case the optical emission from the reverse shock drops to zero very rapidly soon after the reverse shock has crossed the ejecta and the cooling frequency drops below the optical and there are no electrons left to radiate in

the optical band [88].

That said, a few persuasive observations of reverse-shock optical emission have been made in the *Swift* era, so it can finally be said that GRB 990123 does not stand alone. The early optical/IR emission from GRB 041219 would have rivalled that seen from GRB 990123 if not for the large Galactic extinction along the line of sight [36], and of the three distinct peaks observed by PAIRITEL, the second may represent a reverse shock contribution [37] – if so, a relatively small Lorentz factor, $\Gamma \lesssim 70$, is implied. Observations of GRB 050525A with UVOT [89] and GRB 060111B with TAROT (in a unique time-resolved tracking mode; [40]) show the "flattening" light-curve familiar from GRB 021211 (as well as, probably, GRB 990123) that is termed the "type II" light curve by [75]. Evolution of the optical flux in this manner is supposed to indicate the presence of magnetized ejecta or a Poynting-flux dominated outflow.

An alternate case may be provided by GRB 060117, observed by the FRAM sky monitor telescope of the Pierre Auger Observatory [39]. This burst is the largest-fluence GRB observed by *Swift* to-date, and its optical flash was also very bright, peaking at $R \approx 10$ mag and thus rivalling GRB 990123. Although their quality is not high, the data suggest that the forward shock peak is distinguished above the decay of the reverse shock flux, providing a potential first example of the "type I" two-peaked lightcurve that is predicted for a hydrodynamic (nonmagnetized) outflow [75].

Finally, the most exciting prompt robotic IR detection (and optical non-detection) is that of GRB 050904 [18, 16], which is also though to be due to a reverse shock [90, 91] (see, however, [92]). This object, at the unprecedented "very high" redshift of $z = 6.29$ [11], had an X-ray brightness exceeding for a day that of the brightest X-ray quasars [17], and its optical/IR brightness in the first 500 s (observer time) was comparable to that of GRB 990123, with a similarly steep time-decay slope $\alpha \sim 3$.

3. Early Afterglow Models

The afterglow generally becomes important after a time

$$t_{ag} = \mathrm{Max}[(r_{dec}/2c\Gamma^2)(1+z)\ ,\ T] = \mathrm{Max}[10^2 (E_{52}/n_0)^{1/3} \Gamma_2^{-8/3} (1+z)|\mathrm{s}\ ,\ T]\ , \quad (1)$$

where the deceleration time is $t_{dec} \sim (r_{dec}/2c\Gamma^2)$ and T is the duration of the prompt outflow; t_{ag} then marks the beginning of the self-similar blast-wave regime where $\Gamma \propto r^{-3/2} \propto t^{-3/8}$ (in the adiabatic regime; $\Gamma \propto r^{-3} \propto t^{-3/7}$ in the radiative regime).

Denoting the frequency and time dependence of the afterglow spectral energy flux as $F_\nu(t) \propto \nu^{-\beta} t^{-\alpha}$, the late X-ray afterglow phases (3) and (4) described above are similar to those known previously from *Beppo-SAX* (for a review of this earlier behavior and its modeling see e.g. [93]). The "normal" decay phase (3), with temporal decay indices $\alpha \sim 1.1 - 1.5$ and spectral energy indices $\beta \sim 0.7 - 1.0$, is what is expected from the evolution of the forward shock in the Blandford-McKee self-similar late time regime, under the assumption of synchrotron emission.

The late steep decay phase (4) of §1, occasionally seen in *Swift* bursts, is naturally explained as a jet break, when the decrease of the ejecta Lorentz factor leads to the

light-cone angle becoming larger than the jet angular extent, $\Gamma_j(t) \gtrsim 1/\theta_j$ (e.g. [93]). It is noteworthy, however, that this final steepening has been seen in less than $\sim 10\%$ of the *Swift* afterglows, and even then for the most part only in X-rays. The corresponding optical light curve breaks have been few, and not well-constrained. This is unlike the case with the ~ 20 *Beppo-SAX* bursts, for which many achromatic breaks were reported in the optical [94], while in some of the rare cases where an X-ray or radio break was reported it occurred at a different time [95]. The relative paucity of optical breaks in *Swift* afterglows may be an observational selection effect due to the larger median redshift, and hence fainter and redder optical afterglows at the same observer epoch, as well as perhaps reluctance to commit large telescope time on the more frequently-reported *Swift* bursts (an average, roughly, of two per month with *Beppo-SAX* versus two per week with *Swift*).

3.1. Steep Decay

Among the new early afterglow features detected by *Swift*, the steep initial decay phase $F_\nu \propto t^{-3} - t^{-5}$ in X-rays of the long GRB afterglows is one of the most puzzling. There could be several possible reasons for this. The most immediate of these would be the cooling following cessation of the prompt emission (internal shocks or dissipation). If the comoving magnetic field in the emission region is random [or transverse], the flux per unit frequency along the line of sight in a given energy band, as a function of the electron energy index p, decays as $F_\nu \propto t^{-\alpha}$ with $\alpha = -2p$ $[(1-3p)/2]$ in the slow cooling regime, where $\beta = (p-1)/2$, and it decays as $\alpha = -2(1+p)$, $[-(2-3p)/2]$ in the fast cooling regime where $\beta = p/2$, i.e. for the standard $p = 2.5$ this would be $\alpha = -5$, $[-3.25]$ in the slow cooling or $\alpha = -7$, $[-2.75]$ in the fast cooling regime, for random [transverse] fields [71]. In some bursts this may be the explanation, but in others the time and spectral indices do not correspond well.

Currently the most widely considered explanation for the fast decay, either in the initial phase (1) or in the steep flares, attributes it to off-axis emission from regions at $\theta > \Gamma^{-1}$ (also termed curvature effects or high-latitude emission [96]). In this case, after line-of-sight gamma-ray emission has ceased, the off-axis emission observed from $\theta > \Gamma^{-1}$ is $(\Gamma\theta)^{-6}$ smaller than that from the line of sight. Integrating over the equal arrival time region, this flux ratio becomes $\propto (\Gamma\theta)^{-4}$. Since the emission from θ arrives $(\Gamma\theta)^2$ later than from $\theta = 0$, the observer sees the flux falling as $F_\nu \propto t^{-2}$, if the flux were frequency independent. For a source-frame flux $\propto \nu'^{-\beta}$, the observed flux per unit frequency varies then as

$$F_\nu \propto (t - t_0)^{-2-\beta} \tag{2}$$

i.e. $\alpha = 2 + \beta$. This high-latitude radiation, which for observers outside the line cone at $\theta > \Gamma^{-1}$ would appear as prompt γ-ray emission from dissipation at radius r, appears to observers along the line of sight (inside the light cone) to arrive delayed by $t \sim r\theta^2/2c$) relative to the trigger time, and its spectrum is softened by a Doppler factor $D \propto t^{-1}$ into the X-ray observer band. For the initial prompt decay, the onset of the afterglow

(e.g. phases 2 or 3), which also comes from the line of sight, may overlap in time with the delayed high-latitude emission. In equation (2) t_0 can be taken as the trigger time, or some value comparable or less than by equation (1). This can be used to constrain the prompt emission radius [97]. When $t_{dec} < T$, the emission can have an admixture of high-latitude and afterglow contributions, and since the afterglow has a steeper spectrum than the high-latitude emission (which has a prompt spectrum), one can have steeper decays [98]. Values of t_0 closer to the onset of the decay also lead to steeper slopes. Structured jets, when viewed on-beam, produce essentially the same slopes as homogeneous jets, while off-beam observing can lead to shallower slopes [99]. For the flares, if their origin is assumed to be internal (e.g. some form of late internal shock or dissipation) the value of t_0 is just before the flare, near the observed time of flare onset [100]. This interpretation appears, so far, compatible with most of the *Swift* afterglows [15, 14, 101].

Alternatively, the initial fast decay could be due to the emission of a cocoon of exhaust gas [102], where the temporal and spectral index are explained through an approximately power-law behavior of escape times and spectral modification of multiply-scattered photons. The fast decay may also be due to the reverse shock emission, if inverse Compton interactions up-scatter the (primarily synchrotron) optical photons into the X-ray range. The decay starts after the reverse shock has crossed the ejecta and electrons are no longer accelerated, and may have both line-of-sight and off-axis components [103]. This poses strong constraints on the Compton y parameter, and cannot explain steeper decays with $\alpha > 2$, or $\alpha > 2 + \beta$ if the off-axis contribution dominates. Models involving bullets – whose origin, acceleration and survivability is unexplained – could give a prompt decay index $\alpha = 3$ to 5 [104], but imply a bremsstrahlung energy index $\beta \sim 0$ which is not observed in the fast decay, and require fine-tuning. Finally, a "patchy shell" model, where the Lorentz factor is highly variable in angle, would produce emission with $\alpha \sim 2.5$. Thus, such mechanisms may explain the more gradual decays, but not the more extreme $\alpha = 5$ to 7 values encountered in some cases.

3.2. Shallow Decay

The slow decay portion of the X-ray light curves ($\alpha \sim 0.3$ to 0.7), quite ubiquitously detected by *Swift*, is not entirely new, having been detected in a few cases by *Beppo-SAX*. This, as well as the appearance of wiggles and flares in the X-ray light curves several hours after the burst, were the motivation for the "refreshed shocks" scenario [105, 106]. Refreshed shocks can flatten the afterglow light curve for hours or days, even if the ejecta is all emitted promptly at $t = T \lesssim t_\gamma$, but with a range of Lorentz factors, say $M(\Gamma) \propto \Gamma^{-s}$, where the lower Γ shells arrive much later to the foremost fast shells which have already been decelerated. Thus, for an external medium of density $\rho \propto r^{-g}$ and a prompt injection where the Lorentz factor spread relative to ejecta mass and energy is $M(\Gamma) \propto \Gamma^{-s}$, $E(\Gamma) \propto \Gamma^{-s+1}$, the forward shock flux temporal decay is

given by [106]

$$\alpha = [(g-4)(1+s) + \beta(24 - 7g + sg)]/[2(7+s-2g)] \ . \quad (3)$$

It needs to be emphasized that in this model all the ejection can be prompt (e.g. over the duration $\sim T$ of the gamma ray emission) but the low Γ portions arrive at (and refresh) the forward shock at late times, which can range from hours to days. That is, it is not the central engine which is active late; rather, its effects are seen late. Fitting such refreshed-shock models to the shallow decay phases in *Swift* bursts [107] leads to a Γ distribution which is a broken power law, extending above and below a peak around ~ 45.

An alternate version of refreshed shocks does envisage central engine activity extending for long periods of time, e.g. $\lesssim$ day (in contrast to the $\lesssim$ minutes engine activity in the model above). Such long-lived activity may be due to continued fall-back into the central black hole [108] or to a magnetar wind [109]. One characteristic of both types of refreshed models is that after the refreshed shocks stop and the usual decay resumes, the flux level shows a step-up relative to the previous level, since new energy has been injected.

From current analyses, the refreshed shock model is generally able to explain the flatter temporal X-ray slopes seen by *Swift*, both when it is seen to join smoothly on the prompt emission (i.e. without an initial steep decay phase) or when seen after an initial steep decay. Questions remain concerning the interpretation of the fluence ratio in the shallow X-ray afterglow and the prompt gamma-ray emission, which can reach $E_{\rm X}/E_\gamma \lesssim 1$ [98]. This requires a higher radiative efficiency in the prompt gamma-ray emission than in the X-ray afterglow. One could speculate that this might be achieved if the prompt outflow were Poynting-dominated. Alternatively, a highly-efficient afterglow might emit a large fraction of its energy in other (unobserved) bands, e.g. in the GeV or IR. Or [110] a previous mass ejection might have emptied a cavity into which the ejecta moves, leading to greater efficiency at later times, or otherwise causing the energy fraction going into electrons to increase $\propto t^{1/2}$.

3.3. X-ray Flares

Refreshed shocks can also explain some of the X-ray flares whose rise and decay slopes are not too steep. However, this model encounters difficulties with the very steep flares with rise or decay indices $\alpha \sim \pm(5 - -7)$, such as inferred from the giant flare of GRB 050502b [111] around 300 s after the trigger. Also, the flux level increase in this flare is a factor $\sim$ 500 above the smooth afterglow before and after it, implying a comparable energy excess in the low- versus high-Γ material. An explanation based on inverse Compton scattering in the reverse shock [103] can explain a single flare at the beginning of the afterglow, as long as the subsequent flux decay is not too steep. For multiple flares, models invoking blastwave interaction with a lumpy external medium have generic difficulties explaining steep rises and decays [15], although extremely dense, sharp-edged lumps, if they exist, might satisfy the steepness criterion [112].

Currently the more widely-considered model for the flares ascribes them to late central engine activity [15, 14, 101]. The strongest arguments in favor of this are that the energy budget is more easily satisfied, and the fast rises and decays more straightforward to explain. In such a model the flare energy can be comparable to the prompt emission, and the fast rise comes naturally from the short time variability leading to internal shocks (or to rapid reconnection), while the rapid decay may be explained as the high-latitude emission following the flare, with t_0 reset to the beginning of each flare (see discussion in [100]). Considering the full population of X-ray flares, some are well-modeled by refreshed forward shocks, while in others this is clearly ruled out and a central engine origin is better suited [113]. Aside from the phenomenological desirability based on energetics and timescales, a central engine origin is conceivable, within certain time ranges, based on numerical models of the core collapse scenario for long bursts. These invoke the core collapse of a massive stellar progenitor, where continued infall into the fast-rotating core can continue for a long time [108]. However, large flares with a fluence which is a sizable fraction of the prompt emission occurring hours later remain difficult to understand. It has been argued that gravitational instabilities in the infalling debris torus can lead to lumpy accretion [114]. Alternatively, if the accreting debris torus is dominated by magneto-hydrodynamic (MHD) effects, magnetic instabilities can lead to extended, highly time-variable accretion [115].

3.4. Short Burst Afterglows

Swift and to a lesser extent *HETE-2* have provided the first bonafide short burst afterglows, with the first observations beginning (in some cases) within <100 s of the trigger, leading in turn to arcsec and sub-arcsec localizations, host galaxy identifications, and redshifts (although, as yet, none via direct absorption spectroscopy).

In the first short burst afterglow, GRB 050509b [25], the extrapolation of the prompt BAT emission into the X-ray range, along with the XRT light curve from 100 to 1000 s, can be fitted with a single power law of $\alpha \sim 1.2$. The X-ray coverage was sparse due to orbital constraints and the faintness of the afterglow, and the number of detected X-ray photons was small. No optical transient was detected, but an elliptical host galaxy was identified at $z = 0.225$ (e.g. [21]). In GRB 050709 an optical transient was identified, as well as a host galaxy [116], an irregular galaxy at $z = 0.16$ (observations also ruled out any supernova association).

GRB 050724 was relatively bright, and in addition to an X-ray afterglow observed with the XRT and *Chandra* [26], yielded decaying optical and radio afterglows [117]. This burst, as with roughly half the short burst afterglows seen to-date, is associated with an elliptical host galaxy. It also had a low-luminosity, soft gamma-ray extension of the short-hard gamma-ray component (which would have been missed by BATSE), and it had an interesting X-ray afterglow extending beyond 10^5 s, with no jet break seen to the limits of the final *Chandra* observation [27]. The soft gamma-ray extension, lasting up to 200 s, connects smoothly with the beginning of the XRT afterglow, which

has $\alpha \sim 2$ between 100 and 300 s, and then enters a much steeper decay with $\alpha \sim 5$ to 7 out to $\sim 600s$, followed by a more moderate decay $\alpha \sim 1$. An unexpected feature is a strong flare peaking at 5×10^4 s, with an energy 10% that of the prompt emission, and an amplitude which represents a 10-fold increase over the preceding slow decay.

GRB 051221A, the next panchromatic short burst afterglow, has an extended light curve in the X-ray [28] and optical [22]. This was the brightest short burst observed by *Swift* to date, and occurred in a star-forming galaxy at redshift $z = 0.5464$. The X-ray light curve also provides the clearest evidence of "standard" energy injection, with a flattening from 1.4 to 3.4 hours after the burst which increases the afterglow energy by a factor of $\sim$3, and is moreover reflected in contemporaneous radio detections from the VLA.

With seven afterglows and five relatively secure redshifts in hand via host galaxy identifications, the distribution of short bursts in redshift and among host galaxy types – including an equal number of spiral/irregular and elliptical hosts – is typical of an old ($\gtrsim$Gyr) population of progenitors, such as neutron star (NS) binaries or black hole-neutron star binaries [118].

The main challenges posed by the short burst afterglows are the relatively long, soft tail of the prompt emission, and the strength and late occurrence of the flares. A possible explanation for the extended long soft tails ($\sim$100 s) may be that the compact binary progenitor is a black hole - neutron star system [26], since analytical and numerical arguments ([119], and references therein) suggest that disruption of the NS and its disappearance into the black hole may lead to a complex and extended accretion phase significantly longer than for double neutron stars. The flares, for which the simplest interpretation might be as refreshed shocks (compatible with a short engine duration $T \lesssim t_\gamma \sim 2$ s, for ejecta with an extended Lorentz factor distribution), require the energy in the slow material to be at least ten times more energetic than the fast material responsible for the prompt emission in the specific case of the GRB 050724 flare at 10^4 s. The rise and decay times are moderate enough for this interpretation. Another interpretation invokes the accretion-induced collapse of a neutron star in a binary, leading to a flare when the fireball created by the collapse hits the companion [120], which might explain moderate energy one-time flares. However, for repeated, energetic flares, as also seen from long bursts, the total energetics are easier to satisfy if one postulates late central engine activity (lasting at least half a day), containing $\sim$ 10% of the prompt fluence [26]. A possible way to produce this might be via temporary "choking" of an MHD outflow [115] (c.f. [121]), which might imply linear polarization of the X-ray flare [122]. Such MHD effects could plausibly also explain the initial $\sim$100 s soft tail. However, a justification for substantial $\gtrsim 10^5$ s features remains so far on tentative grounds.

The similarity of the X-ray afterglow light curves to those of long bursts is, in itself, an argument in favor of the prevalent view that the afterglows of both long and short bursts can be described by the same paradigm, independently of any differences in the progenitors. This impression is reinforced by the fact that the X-ray light curve

temporal slope is, on average, that expected from the usual forward shock afterglow model, and that in two short bursts (so far) there is evidence for what appears to be a jet break [116, 28, 22]. However, while very similar, the first-order differences are revealing: the average isotropic energy of the short bursts is a factor of ∼100 smaller, while the average jet opening angle (based on two breaks and one lower limit) is a factor of ∼ 2 larger [116, 27, 28, 22]. Using the standard afterglow theory, the bulk Lorentz factor decay can be expressed through $\Gamma(t_d) = 6.5(n_o/E_{50})^{1/8} t_d^{-3/8}$, where $t_d = (t/\mathrm{day})$, n_o is the external density in units of cm^{-3}, and E_{50} is the isotropic equivalent energy in units of 10^{50} erg. If the jet break occurs at $\Gamma(t_{br}) = \theta_j^{-1}$ the jet opening angle and the total jet energy E_j are

$$\theta_j = 9^o (n_o/E_{50})^{1/8} t_{d,br}^{3/8} \ , E_j = \pi \theta_j^2 E \sim 10^{49} n_o^{1/4} (E_{50} t_{d,br})^{3/4} \ \mathrm{erg} \ . \qquad (4)$$

For the first three well-studied afterglows, GRBs 050709, 050724, and 051221A, these equations, together with the standard afterglow expressions for the flux level as a function of time before and after the break, lead to fits [123, 28, 22] which are not completely determined, allowing for GRBs 050709 and 051221A either a very low or a moderately low external density, and for GRB 050724 a moderately low to large external density. The main uncertainties are in the jet break times, which are poorly sampled, and in the absence of high-quality radio data for any burst (GRB 050724 had a reasonable radio flux, but too much variability in all bands). More bright short bursts like GRB 051221A will be needed to improve the jet break statistics substantially.

3.5. The Supernova Component

GRB-associated supernovae have been regularly observed as "red bumps" in the light curves of low-redshift GRBs, and more rarely, by direct spectroscopic observation at 7 to 30 days after the GRB.

The observation of the GRB-supernova GRB 060218/SN 2006aj with *Swift*, however, has raised the prospect of an entirely new component of emission at early times, namely, the shock breakout of the simultaneous supernova explosion. The thermal component of the prompt XRT emission, which evolves into the UVOT range over the course of the first few hours after the burst, has been interpreted as the shock break-out of the GRB/SN in an optically-thick wind of a Wolf-Rayet progenitor star [29] (but see also [34]). It is important that the wind be sufficiently dense; given the known redshift of this burst, the blackbody radius of the early XRT/UVOT thermal component is roughly 100 times the size of a Wolf-Rayet star. At the same time, however, the absence of hydrogen features (e.g. Hα) in the SN spectrum requires such a progenitor, and disallows a red giant progenitor, which would produce a type II SN.

The observation of a single such event in one year of *Swift* observations offers the tantalizing prospect of gathering more examples with each additional year of *Swift* operations. In particular, intensive ground-based observations tracking the evolution of this thermal component to near-infrared, millimeter, and radio wavelengths will be useful in confirming or refuting the shock-breakout interpretation.

Acknowledgements: We are grateful to the *Swift* team for collaborations and to NSF AST 0307376 and NASA NAG5 13286 for support. We thank Lijun Gou for preparation of Figure 2.

References

[1] Gehrels, N. et al. The Swift Gamma-Ray Burst Mission. ApJ 611, 1005–1020, August (2004).

[2] Barthelmy, S. D. et al. The Burst Alert Telescope (BAT) on the SWIFT Midex Mission. *Space Science Reviews* 120, 143–164, October (2005).

[3] Band, D. L. Postlaunch Analysis of Swift's Gamma-Ray Burst Detection Sensitivity. ApJ 644, 378–384, June (2006).

[4] Burrows, D. N. et al. The Swift X-Ray Telescope. *Space Science Reviews* 120, 165–195, October (2005).

[5] Roming, P. W. A. et al. The Swift Ultra-Violet/Optical Telescope. In X-Ray and Gamma-Ray Instrumentation for Astronomy XIII. Edited by Flanagan, Kathryn A.; Siegmund, Oswald H. W. Proceedings of the SPIE, Volume 5165, pp. 262-276 (2004)., Flanagan, K. A. and Siegmund, O. H. W., editors, 262–276, , February (2004).

[6] Burrows, D. N. et al. Swift XRT Observations of X-ray Flares in GRB Afterglows. *ArXiv.org* astro-ph/0511039, 1+, November (2005).

[7] Roming, P. W. A. et al. Suppression of the Early Optical Afterglow of Gamma-Ray Bursts. *ArXiv.org* astro-ph/0509273, 1+, September (2005).

[8] Jakobsson, P. et al. GRB 050814 at z = 5.3 and the Redshift Distribution of Swift GRBs. *ArXiv.org* astro-ph/0602071, 1+, February (2006).

[9] Bagoly, Z. et al. The Swift satellite and redshifts of long gamma-ray bursts. *ArXiv.org* astro-ph/0604326, 1+, April (2006).

[10] Berger, E. et al. Afterglows, Redshifts, and Properties of Swift Gamma-Ray Bursts. ApJ 634, 501–508, November (2005).

[11] Kawai, N. et al. Afterglow spectrum of a gamma-ray burst with the highest known redshift z=6.295. *ArXiv.org* astro-ph/0512052, 1+, December (2005).

[12] Andersen, M. I. et al. VLT identification of the optical afterglow of the gamma-ray burst GRB 000131 at z=4.50. A&A 364, L54–L61, December (2000).

[13] Gehrels, N. The Swift Gamma-Ray Burst Mission. In AIP Conf. Proc.: Gamma-Ray Bursts in the Swift Era, Holt, S. S., Gehrels, N., and Nousek, J., editors, 1+, , September (2006).

[14] Nousek, J. A. et al. Evidence for a Canonical Gamma-Ray Burst Afterglow Light Curve in the Swift XRT Data. ApJ 642, 389–400, May (2006).

[15] Zhang, B., Fan, Y. Z., Dyks, J., Kobayashi, S., Mészáros, P., Burrows, D. N., Nousek, J. A., and Gehrels, N. Physical Processes Shaping Gamma-Ray Burst X-Ray Afterglow Light Curves: Theoretical Implications from the Swift X-Ray Telescope Observations. ApJ 642, 354–370, May (2006).

[16] Haislip, J. B. et al. A photometric redshift of z = 6.39 ± 0.12 for GRB 050904. Nature 440, 181–183, March (2006).

[17] Watson, D. et al. Outshining the Quasars at Reionization: The X-Ray Spectrum and Light Curveof the Redshift 6.29 Gamma-Ray Burst GRB 050904. ApJ 637, L69–L72, February (2006).

[18] Boër, M., Atteia, J. L., Damerdji, Y., Gendre, B., Klotz, A., and Stratta, G. Detection of a Very Bright Optical Flare from the Gamma-Ray Burst GRB 050904 at Redshift 6.29. ApJ 638, L71–L74, February (2006).

[19] Cusumano, G. et al. Gamma-ray bursts: Huge explosion in the early Universe. Nature 440, 164–+, March (2006).

[20] Tagliaferri, G. et al. GRB 050904 at redshift 6.3: observations of the oldest cosmic explosion after the Big Bang. A&A 443, L1–L5, November (2005).

[21] Berger, E. The Afterglows and Host Galaxies of Short GRBs: An Overview. In AIP Conf. Proc.: Gamma-Ray Bursts in the Swift Era, Holt, S. S., Gehrels, N., and Nousek, J., editors, 1+, , September (2006).

[22] Soderberg, A. M. et al. The Afterglow, Energetics and Host Galaxy of the Short-Hard Gamma-Ray Burst 051221a. *ArXiv.org* astro-ph/0601455, January (2006).

[23] Prochaska, J. X. et al. The Galaxy Hosts and Large-Scale Environments of Short-Hard Gamma-Ray Bursts. ApJ 642, 989–994, May (2006).

[24] de Ugarte Postigo, A. et al. GRB 060121: Implications of a Short/Intermediate Duration Gamma-Ray Burst at High Redshift. *ArXiv.org* astro-ph/0605516, 1+, May (2006).

[25] Gehrels, N. et al. A short γ-ray burst apparently associated with an elliptical galaxy at redshift z = 0.225. Nature 437, 851–854, October (2005).

[26] Barthelmy, S. D. et al. An origin for short γ-ray bursts unassociated with current star formation. Nature 438, 994–996, December (2005).

[27] Grupe, D., Burrows, D. N., Patel, S. K., Kouveliotou, C., Zhang, B., Meszaros, P., Wijers, R. A. M., and Gehrels, N. Jet Breaks in Short Gamma-Ray Bursts. I: The Uncollimated Afterglow of GRB 050724. *ArXiv.org* astro-ph/0603773, 1+, March (2006).

[28] Burrows, D. N. et al. Jet Breaks in Short Gamma-Ray Bursts. II: The Collimated Afterglow of GRB 051221A. *ArXiv.org* astro-ph/0604320, 1+, April (2006).

[29] Campana, S. et al. The shock break-out of GRB 060218/SN 2006aj. *ArXiv.org* astro-ph/0603279, 1+, March (2006).

[30] Modjaz, M. et al. Early-Time Photometry and Spectroscopy of the Fast Evolving SN 2006AJ Associated with GRB 060218. *ArXiv.org* astro-ph/0603377, 1+, March (2006).

[31] Mirabal, N., Halpern, J. P., An, D., Thorstensen, J. R., and Terndrup, D. M. GRB 060218/SN 2006aj: A Gamma-Ray Burst and Prompt Supernova at z = 0.0335. ApJ 643, L99–L102, June (2006).

[32] Pian, E. et al. . An optical supernova associated with the X-ray flash XRF 060218. *ArXiv.org* astro-ph/0603530, 1+, March (2006).

[33] Soderberg, A. M. et al. Relativistic ejecta from XRF 060218 and the complete census of cosmic explosions. *ArXiv.org* astro-ph/0604389, 1+, April (2006).

[34] Fan, Y., Piran, T., and Xu, D. The Interpretation and Implication of the Afterglow of GRB 060218. *ArXiv.org* astro-ph/0604016, 1+, April (2006).

[35] Della Valle, M. et al. Hypernova Signatures in the Late Rebrightening of GRB 050525A. ApJ 642, L103–L106, May (2006).

[36] Vestrand, W. T. et al. A link between prompt optical and prompt γ-ray emission in γ-ray bursts. Nature 435, 178–180, May (2005).

[37] Blake, C. H. et al. An infrared flash contemporaneous with the γ-rays of GRB 041219a. Nature 435, 181–184, May (2005).

[38] Vestrand, W. T. et al. Energy input and response from prompt and early optical afterglow emission in gamma-ray bursts. *ArXiv.org* astro-ph/0605472, 1+, May (2006).

[39] Jelínek, M. et al. The bright optical flash from GRB 060117. *ArXiv.org* astro-ph/0606004, 1+, June (2006).

[40] Klotz, A., Gendre, B., Stratta, G., Atteia, J. L., Boër, M., Malacrino, F., Damerdji, Y., and Behrend, R. Continuous optical monitoring during the prompt emission of GRB 060111B. A&A 451, L39–L42, June (2006).

[41] Band, D. et al. BATSE observations of gamma-ray burst spectra. I - Spectral diversity. ApJ 413, 281–292, August (1993).

[42] Ryde, F. The Cooling Behavior of Thermal Pulses in Gamma-Ray Bursts. ApJ 614, 827–846, October (2004).

[43] Meszaros, P. and Rees, M. J. Relativistic fireballs and their impact on external matter - Models for cosmological gamma-ray bursts. ApJ 405, 278–284, March (1993).

[44] Meszaros, P. and Rees, M. J. Gamma-Ray Bursts: Multiwaveband Spectral Predictions for Blast Wave Models. ApJ 418, L59+, December (1993).

[45] Medvedev, M. V. and Loeb, A. Generation of Magnetic Fields in the Relativistic Shock of Gamma-Ray Burst Sources. ApJ 526, 697–706, December (1999).

[46] Medvedev, M. V., Silva, L. O., Fiore, M., Fonseca, R. A., and Mori, W. B. Generation of Magnetic Fields in Cosmological Shocks. *Journal of Korean Astronomical Society* 37, 533–541, December (2004).

[47] Spitkovsky, A. Simulations of relativistic collisionless shocks: shock structure and particle acceleration. In AIP Conf. Proc. 801: Astrophysical Sources of High Energy Particles and Radiation, Bulik, T., Rudak, B., and Madejski, G., editors, 345–350, , November (2005).

[48] Rees, M. J. and Meszaros, P. Unsteady outflow models for cosmological gamma-ray bursts. ApJ 430, L93–L96, August (1994).

[49] Meszaros, P., Rees, M. J., and Papathanassiou, H. Spectral properties of blast-wave models of gamma-ray burst sources. ApJ 432, 181–193, September (1994).

[50] Sari, R., Piran, T., and Narayan, R. Spectra and Light Curves of Gamma-Ray Burst Afterglows. ApJ 497, L17+, April (1998).

[51] Granot, J., Piran, T., and Sari, R. Synchrotron Self-Absorption in Gamma-Ray Burst Afterglow. ApJ 527, 236–246, December (1999).

[52] Dermer, C. D., Chiang, J., and Mitman, K. E. Beaming, Baryon Loading, and the Synchrotron Self-Compton Component in Gamma-Ray Bursts. ApJ 537, 785–795, July (2000).

[53] Preece, R. D., Briggs, M. S., Mallozzi, R. S., Pendleton, G. N., Paciesas, W. S., and Band, D. L. The BATSE Gamma-Ray Burst Spectral Catalog. I. High Time Resolution Spectroscopy of Bright Bursts Using High Energy Resolution Data. ApJS 126, 19–36, January (2000).

[54] Granot, J., Piran, T., and Sari, R. The Synchrotron Spectrum of Fast Cooling Electrons Revisited. ApJ 534, L163–L166, May (2000).

[55] Panaitescu, A. and Mészáros, P. Gamma-Ray Bursts from Upscattered Self-absorbed Synchrotron Emission. ApJ 544, L17–L21, November (2000).

[56] Medvedev, M. V. Theory of "Jitter" Radiation from Small-Scale Random Magnetic Fields and Prompt Emission from Gamma-Ray Burst Shocks. ApJ 540, 704–714, September (2000).

[57] Medvedev, M. V. The Theory of Spectral Evolution of the Gamma-Ray Burst Prompt Emission. ApJ 637, 869–872, February (2006).

[58] Lloyd, N. M. and Petrosian, V. Synchrotron Radiation as the Source of Gamma-Ray Burst Spectra. ApJ 543, 722–732, November (2000).

[59] Lloyd-Ronning, N. M. and Petrosian, V. Interpreting the Behavior of Time-resolved Gamma-Ray Burst Spectra. ApJ 565, 182–194, January (2002).

[60] Mészáros, P. and Rees, M. J. Steep Slopes and Preferred Breaks in Gamma-Ray Burst Spectra: The Role of Photospheres and Comptonization. ApJ 530, 292–298, February (2000).

[61] Pe'er, A. and Waxman, E. Prompt Gamma-Ray Burst Spectra: Detailed Calculations and the Effect of Pair Production. ApJ 613, 448–459, September (2004).

[62] Pe'er, A. and Waxman, E. Time-dependent Numerical Model for the Emission of Radiation from Relativistic Plasma. ApJ 628, 857–866, August (2005).

[63] Rees, M. J. and Mészáros, P. Dissipative Photosphere Models of Gamma-Ray Bursts and X-Ray Flashes. ApJ 628, 847–852, August (2005).

[64] Pe'er, A., Mészáros, P., and Rees, M. J. Peak Energy Clustering and Efficiency in Compact Objects. ApJ 635, 476–480, December (2005).

[65] Pe'er, A., Mészáros, P., and Rees, M. J. The Observable Effects of a Photospheric Component on GRB and XRF Prompt Emission Spectrum. ApJ 642, 995–1003, May (2006).

[66] Amati, L. et al. Intrinsic spectra and energetics of BeppoSAX Gamma-Ray Bursts with known redshifts. A&A 390, 81–89, July (2002).

[67] Ghirlanda, G., Ghisellini, G., and Lazzati, D. The Collimation-corrected Gamma-Ray Burst Energies Correlate with the Peak Energy of Their νF_ν Spectrum. ApJ 616, 331–338, November (2004).

[68] Thompson, C. Deceleration of a Relativistic, Photon-Rich Shell: End of Preacceleration, Damping of MHD Turbulence, and the Emission Mechanism of Gamma-Ray Bursts. *ArXiv.org* astro-ph/0507387, 1+, July (2005).

[69] Akerlof, C. et al. Observation of contemporaneous optical radiation from a gamma-ray burst. Nature 398, 400–402 (1999).

[70] Sari, R. and Piran, T. GRB 990123: The Optical Flash and the Fireball Model. ApJ 517, L109–L112, June (1999).

[71] Mészáros, P. and Rees, M. J. GRB 990123: reverse and internal shock flashes and late afterglow behaviour. MNRAS 306, L39–L43, July (1999).

[72] Nakar, E. and Piran, T. GRB 990123 Revisited: Further Evidence of a Reverse Shock. ApJ 619, L147–L150, February (2005).

[73] Meszaros, P. and Rees, M. J. Optical and Long-Wavelength Afterglow from Gamma-Ray Bursts. ApJ 476, 232–+, February (1997).

[74] Kobayashi, S. and Zhang, B. GRB 021004: Reverse Shock Emission. ApJ 582, L75–L78, January (2003).

[75] Zhang, B., Kobayashi, S., and Mészáros, P. Gamma-Ray Burst Early Optical Afterglows: Implications for the Initial Lorentz Factor and the Central Engine. ApJ 595, 950–954, October (2003).

[76] Fox, D. W. et al. Early optical emission from the γ-ray burst of 4 October 2002. Nature 422, 284–286, March (2003).

[77] Fox, D. W. et al. Discovery of Early Optical Emission from GRB 021211. ApJ 586, L5–L8, March (2003).

[78] Li, W., Filippenko, A. V., Chornock, R., and Jha, S. The Early Light Curve of the Optical Afterglow of GRB 021211. ApJ 586, L9–L12, March (2003).

[79] Wei, D. M. The afterglow of GRB 021211: Another case of reverse shock emission. A&A 402, L9–L12, April (2003).

[80] Rykoff, E. S. et al. Prompt Optical Detection of GRB 050401 with ROTSE-IIIa. ApJ 631, L121–L124, October (2005).

[81] Quimby, R. M. et al. Early-Time Observations of the GRB 050319 Optical Transient. ApJ 640, 402–406, March (2006).

[82] Yost, S. A. et al. Optical Light Curve and Cooling Break of GRB 050502A. ApJ 636, 959–966, January (2006).

[83] Rykoff, E. S. et al. The Early Optical Afterglow of GRB 030418 and Progenitor Mass Loss. ApJ 601, 1013–1018, February (2004).

[84] Rykoff, E. S. et al. The Anomalous Early Afterglow of GRB 050801. ApJ 638, L5–L8, February (2006).

[85] Kobayashi, S. Light Curves of Gamma-Ray Burst Optical Flashes. ApJ 545, 807–812, December (2000).

[86] Mészáros, P., Ramirez-Ruiz, E., Rees, M. J., and Zhang, B. X-Ray-rich Gamma-Ray Bursts, Photospheres, and Variability. ApJ 578, 812–817, October (2002).

[87] Nakar, E. and Piran, T. Early afterglow emission from a reverse shock as a diagnostic tool for gamma-ray burst outflows. MNRAS 353, 647–653, September (2004).

[88] McMahon, E., Kumar, P., and Piran, T. Reverse shock emission as a probe of gamma-ray burst ejecta. MNRAS 366, 575–585, February (2006).

[89] Blustin, A. J. et al. Swift Panchromatic Observations of the Bright Gamma-Ray Burst GRB 050525a. ApJ 637, 901–913, February (2006).

[90] Fan, Y. Z., Zhang, B., and Wei, D. M. Early Optical-Infrared Emission from GRB 041219a: Neutron-rich Internal Shocks and a Mildly Magnetized External Reverse Shock. ApJ 628, L25–L28, July (2005).

[91] Wei, D. M., Yan, T., and Fan, Y. Z. The Optical Flare and Afterglow Light Curve of GRB 050904 at Redshift z=6.29. ApJ 636, L69–L72, January (2006).

[92] Wei, D. M. The GRB early optical flash from internal shock: application to GRB990123, GRB041219a and GRB060111b. *ArXiv.org* astro-ph/0605016, 1+, April (2006).

[93] Zhang, B. and Mészáros, P. Gamma-Ray Bursts: progress, problems & prospects. *International Journal of Modern Physics A* 19, 2385–2472 (2004).

[94] Frail, D. A. et al. Beaming in Gamma-Ray Bursts: Evidence for a Standard Energy Reservoir. ApJ 562, L55–L58, November (2001).

[95] Berger, E., Kulkarni, S. R., and Frail, D. A. A Standard Kinetic Energy Reservoir in Gamma-Ray Burst Afterglows. ApJ 590, 379–385, June (2003).

[96] Kumar, P. and Panaitescu, A. Steepening of Afterglow Decay for Jets Interacting with Stratified Media. ApJ 541, L9–L12, September (2000).

[97] Lazzati, D. and Begelman, M. C. Thick Fireballs and the Steep Decay in the Early X-Ray Afterglow of Gamma-Ray Bursts. ApJ 641, 972–977, April (2006).

[98] O'Brien, P. T. et al. The early X-ray emission from GRBs. *ArXiv.org* astro-ph/0601125, 1+, January (2006).

[99] Dyks, J., Zhang, B., and Fan, Y. Z. Curvature effect in structured GRB jets. *ArXiv.org* astro-ph/0511699, 1+, November (2005).

[100] Zhang, B. Physical origin of X-ray flares following GRBs. In AIP Conf. Proc.: Gamma-Ray Bursts in the Swift Era, Holt, S. S., Gehrels, N., and Nousek, J., editors, 1+, , September (2006).

[101] Panaitescu, A., Mészáros, P., Gehrels, N., Burrows, D., and Nousek, J. Analysis of the X-ray emission of nine Swift afterglows. MNRAS 366, 1357–1366, March (2006).

[102] Pe'er, A., Mészáros, P., and Rees, M. J. Radiation from an expanding cocoon as an explanation of the steep decay observed in GRB early afterglow light curves. *ArXiv.org* astro-ph/0603343, 1+, March (2006).

[103] Kobayashi, S., Zhang, B., Meszaros, P., and Burrows, D. N. Inverse Compton X-ray Flare from GRB Reverse Shock. *ArXiv.org* astro-ph/0506157, 1+, June (2005).

[104] Dado, S., Dar, A., and De Rujula, A. On the "canonical behaviour" of the X-ray afterglows of the Gamma Ray Bursts observed with Swift's XRT. *ArXiv.org* astro-ph/0512196, 1+, December (2005).

[105] Rees, M. J. and Meszaros, P. Refreshed Shocks and Afterglow Longevity in Gamma-Ray Bursts. ApJ 496, L1+, March (1998).

[106] Sari, R. and Mészáros, P. Impulsive and Varying Injection in Gamma-Ray Burst Afterglows. ApJ 535, L33–L37, May (2000).

[107] Granot, J. and Kumar, P. Distribution of gamma-ray burst ejecta energy with Lorentz factor. MNRAS 366, L13–L16, February (2006).

[108] Woosley, S. and Heger, A. The Supernova Gamma-Ray Burst Connection. In AIP Conf. Proc.: Gamma-Ray Bursts in the Swift Era, Holt, S. S., Gehrels, N., and Nousek, J., editors, 1+, , September (2006).

[109] Zhang, B. and Mészáros, P. Gamma-Ray Burst Afterglow with Continuous Energy Injection: Signature of a Highly Magnetized Millisecond Pulsar. ApJ 552, L35–L38, May (2001).

[110] Ioka, K., Toma, K., Yamazaki, R., and Nakamura, T. Efficiency Crisis of Swift Gamma-Ray Bursts with Shallow X-ray Afterglows: Prior Activity or Time-Dependent Microphysics? *ArXiv.org* astro-ph/0511749, 1+, November (2005).

[111] Burrows, D. N. et al. Bright X-ray Flares in Gamma-Ray Burst Afterglows. *Science* 309, 1833–1835, September (2005).

[112] Dermer, C. X-ray Flares from External Shocks. In AIP Conf. Proc.: Gamma-Ray Bursts in the Swift Era, Holt, S. S., Gehrels, N., and Nousek, J., editors, 1+, , September (2006).

[113] Wu, X. F., Dai, Z. G., Wang, X. Y., Huang, Y. F., Feng, L. L., and Lu, T. X-ray flares: late internal and late external shocks. *ArXiv.org* astro-ph/0512555, 1+, December (2005).

[114] Perna, R., Armitage, P. J., and Zhang, B. Flares in Long and Short Gamma-Ray Bursts: A Common Origin in a Hyperaccreting Accretion Disk. ApJ 636, L29–L32, January (2006).

[115] Proga, D. and Begelman, M. C. Accretion of Low Angular Momentum Material onto Black Holes: Two-dimensional Magnetohydrodynamic Case. ApJ 592, 767–781, August (2003).

[116] Fox, D. B. et al. The afterglow of GRB 050709 and the nature of the short-hard γ-ray bursts. Nature 437, 845–850, October (2005).

[117] Berger, E. et al. A Merger Origin for Short Gamma-Ray Bursts Inferred from the Afterglow and Host Galaxy of GRB 050724. Nature 438, 988–990, December (2005).

[118] Nakar, E., Gal-Yam, A., and Fox, D. B. The Local Rate and the Progenitor Lifetimes of Short-Hard Gamma-Ray Bursts: Synthesis and Predictions for LIGO. *ArXiv.org* astro-ph/0511254, 1+, November (2005).

[119] Davies, M. B., Levan, A. J., and King, A. R. The ultimate outcome of black hole-neutron star mergers. MNRAS 356, 54–58, January (2005).

[120] MacFadyen, A. I., Ramirez-Ruiz, E., and Zhang, W. X-ray flares following short gamma-ray bursts from shock heating of binary stellar companions. *ArXiv.org* astro-ph/0510192, 1+, October (2005).

[121] van Putten, M. H. P. M. and Ostriker, E. C. Hyper- and Suspended-Accretion States of Rotating Black Holes and the Durations of Gamma-Ray Bursts. ApJ 552, L31–L34, May (2001).

[122] Fan, Y. Z., Zhang, B., and Proga, D. Linearly Polarized X-Ray Flares following Short Gamma-Ray Bursts. ApJ 635, L129–L132, December (2005).

[123] Panaitescu, A. The energetics and environment of the short-GRB afterglows 050709 and 050724. MNRAS 367, L42–L46, March (2006).